J. Fluid Mech. (1980), *vol.* 96, *part* 2, *pp.* 395–412
Printed in Great Britain

Curvature effects on hydraulically driven inertial boundary currents

By LARS PETTER RØED
Geophysical Institute Division A,
University of Bergen, Norway

(Received 25 September 1978, and in revised form 6 April 1979)

The idea behind the general theory of 'hydraulic'-type problems as described by Gill (1977) is applied to an inertial boundary current. The flow considered is a single-layer inviscid fluid flowing under gravity along a rotating, irregular wall. It is shown that owing to variations in the curvature of the wall the boundary current may be controlled in the hydraulic sense at sections along the wall classified as 'bays'. It is also shown that because of such variations in geometry the flow can be 'blocked'. The behaviour of the flow in response to variations in the bottom topography, such as a varying lateral slope or a broad-crested weir, is discussed with particular reference to conditions under which the flow is either controlled or blocked.

1. Introduction

Recently there has been a renewed interest in 'hydraulic'-type problems with special emphasis on rotational effects, cf. Stern (1972, 1974, 1976), Whitehead, Leetmaa & Knox (1974), Sambuco & Whitehead (1976), Gill (1977) and Shen (1978). The investigations reported have been directed at the problem adopted from non-rotating hydraulics (Rouse 1961) under which conditions the flow is hydraulically controlled, i.e. to the question of whether a given downstream geometry is sufficient to calculate one of the upstream parameters (such as the discharge rate or upstream height).

In a recent paper Gill (1977) addressed himself to the 'hydraulic'-type problem in fairly general terms and applied the general theory for flow of an inviscid single-layer fluid in a rotating channel for the case of uniform potential vorticity. Because of the rotation the free surface may have quite a large cross-stream tilt. His analysis shows in fact that the flow may be separated from the left wall† upstream. Thus because of rotation there exists a family of possible upstream states where the surface of the fluid intersects the bottom so that the stream occupies only a part of the channel, leaving the remainder of the channel floor dry. For such flows the left wall is superfluous and may be removed, in which case the flow assumes the characteristics of an inertial boundary current.

Although the analysis of Gill (1977) implicitly includes some discussion of an inertial boundary current, he did not address himself to the problem as such. Moreover, important geometrical features, such as curvature of the right wall, which in general

† Left and right is relative to the direction of the mean flow, which also defines the downstream direction.

0022-1120/80/4354-8050 $02.00

require the solution to a nonlinear differential equation, and lateral bottom topography were neglected. It is felt therefore that such features should be included.

The very existence of this boundary current depends on the choice of upstream parameters (of which there are *three* for the case of uniform potential vorticity) and therefore consideration of the upstream state is included in a separate section (§ 3). This section also conveniently serves the purpose of introducing the concepts involved and some of the notation.

The flow to be considered is a *forced* flow, but it has some bearing on the problem of a *free* discharge. If, because of changes in the downstream geometry, a solution to the forced flow does not exist, then in a real flow a shock or other phenomenon beyond the bounds of the theory would presumably occur. However, in a *free* discharge, such a phenomenon may propagate upstream and thereby alter the upstream parameters accordingly (i.e. hydraulic control).

The behaviour of an inertial boundary current in response to coastline irregularities is considered. The analysis reveals that, besides the possibility of controlled flow solutions, regions close to the wall are formed downstream from where the flow is blocked, in the sense that no streamline originating upstream enters this blocked region. For instance, if a unidirectional flow stagnates at the wall, a streamline leaves the wall at this point and a region of reversed flow close to the wall, with streamlines originating downstream, is created. Such a flow is not physically meaningful within the context of the present theory since it necessitates information about the downstream flow. The blocking was not discussed by Gill (1977) since this feature is not present when only topographic variations with downstream distance are considered. Blocking is also recognized if the fluid depth goes to zero at the wall, with the flow separating from the wall downstream of this point. This blocking, however, is purely a matter of description because the distinction between wall and bottom is only meaningful when they intersect.

The flow considered consists of a single-layer inviscid fluid of uniform density flowing under gravity along a rotating irregular, vertical wall and over a varying topography. However, the theory is easily extended to yield results for a two-layer system where one of the layers is quiescent, in which case gravity is replaced by 'reduced gravity' (e.g. Stern 1976). In § 2 the equations for flow in a boundary current relative to a curvilinear co-ordinate system are established. In §§ 4 and 5 the dependence of the flow on bottom topography variations and coastline irregularities is discussed. The flow may be thought to be either a dense body of water flowing along a continental margin underneath a less dense stagnant fluid, or a surface boundary-layer current such as the Norwegian Coastal Current or the East Greenland Current. In § 6 some examples of flow along irregular walls are depicted to help visualize the dependence of the flow variables on wall irregularities.

2. Equations for flow in a boundary current

Consider the case of a homogeneous, incompressible, inviscid fluid bounded laterally by a vertical wall to the right of the direction of the mean flow and which rotates about the vertical axis with uniform angular velocity $\frac{1}{2}f$. The motion will be described relative to a curvilinear co-ordinate system (s, n, z) in the rotating frame, with the z axis pointing vertically upwards and the s and n co-ordinate directions along and

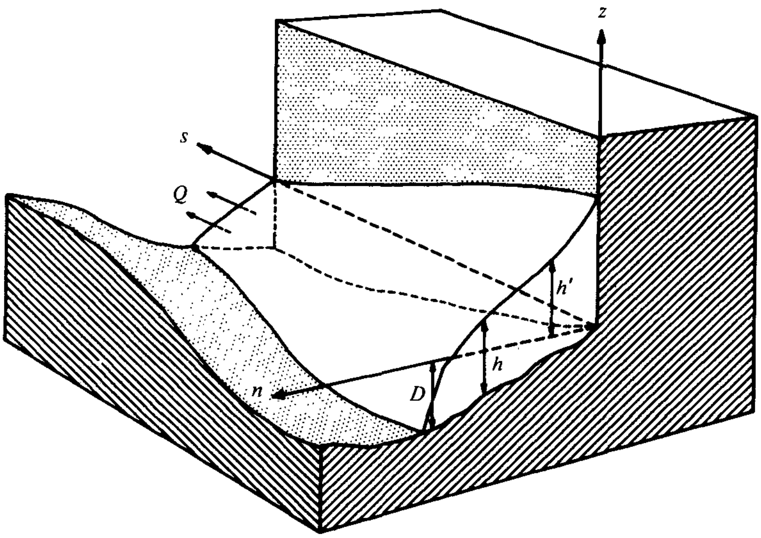

FIGURE 1. Sketch of the co-ordinate system and the symbols used in the text.

normal to the wall respectively. The fluid is bounded by the bottom, $z = -D(s,n)$, and the free surface, $z = h'(s,n)$. Thus the height of a fluid column is

$$h = h' + D. \tag{2.1}$$

A convenient choice of reference level ($z = 0$) is the bottom level far upstream ($s \to -\infty$) at the wall, i.e.

$$D(-\infty, 0) = 0. \tag{2.2}$$

Figure 1 shows the system and the symbols as defined above. The flow will be assumed to be a boundary current and accordingly solutions for h will be sought such that, for a certain lateral distance, $n = w(s)$, from the wall, $h = 0$. The solutions are therefore subject to the condition

$$h_l = h(s, w) = 0, \tag{2.3}$$

where the subscript l from here on denotes evaluation of that quantity at the free streamline, $n = w(s)$. The subscript r will be used to denote evaluation at the supporting wall, $n = 0$. The determination of the position of the free streamline will be an integral part of the problem. The analysis is restricted to the case of uniform potential vorticity and the governing equations are those of Gill (1977). Let g be the gravitational acceleration and u and v the velocities along and normal to the wall, respectively. Then the governing equations take the following form in the curvilinear system:

$$\left(1+\frac{n}{\rho}\right)^{-1} u\frac{\partial u}{\partial s} + v\frac{\partial u}{\partial n} + \frac{uv}{\rho+n} - fv = -g\left(1+\frac{n}{\rho}\right)^{-1}\frac{\partial(h-D)}{\partial s}, \tag{2.4}$$

$$\left(1+\frac{n}{\rho}\right)^{-1} u\frac{\partial v}{\partial s} + v\frac{\partial v}{\partial n} - \frac{u^2}{\rho+n} + fu = -g\frac{\partial(h-D)}{\partial n}, \tag{2.5}$$

$$-\frac{\partial u}{\partial n} + \left(1+\frac{n}{\rho}\right)^{-1}\frac{\partial v}{\partial s} - \frac{u}{\rho+n} + f = fh/H_0 \tag{2.6}$$

and

$$\tfrac{1}{2}(u^2+v^2) + g(h-D) = gH_r + \frac{f}{H_0}(\psi - Q). \tag{2.7}$$

Here ρ is the radius of curvature of the wall and is a function of s only. The sign convention is such that ρ is *positive* at capes and *negative* at bays. Q is the total discharge rate or volume flux. The stream function ψ is defined by

$$hu = -\frac{\partial\psi}{\partial n}, \quad hv = \left(1+\frac{n}{\rho}\right)^{-1}\frac{\partial\psi}{\partial s}, \tag{2.8}$$

such that $\psi = Q$ at the wall and $\psi = 0$ at the free streamline. The constant H_0 is the fluid depth at points where the relative vorticity is zero and the constant H_r the surface elevation at the wall at points where the velocity is zero.

Non-dimensional variables are defined by

$$\left.\begin{aligned}&\hat{s} = s/\lambda_s, \quad \hat{n} = n/w_s, \quad \hat{u} = u/u_s, \quad \hat{v} = v/v_s,\\ &\hat{\rho} = \rho/\rho_s, \quad \hat{\psi} = \psi/Q, \quad \hat{D} = D/D_s, \quad \hat{w} = w/w_s,\\ &\hat{h} = h/D_s,\end{aligned}\right\} \tag{2.9}$$

where

$$w_s = 2(gH_0)^{\frac{1}{2}}/f \tag{2.10}$$

is the Rossby radius of deformation based on the potential vorticity height, H_0. D_s and u_s are depth and velocity scales, respectively, based on mass continuity and geostrophic balance, namely

$$u_s = (\tfrac{1}{2}fQ/H_0)^{\frac{1}{2}}, \quad D_s = (\tfrac{1}{2}fQ/g)^{\frac{1}{2}}. \tag{2.11}$$

A typical absolute value of the radius of curvature is denoted by ρ_s and λ_s is a typical length over which the variables vary with downstream distance. From mass continuity requirements it follows that the relative scaling of u and v is such that

$$\lambda_s v_s = w_s u_s. \tag{2.12}$$

There are four dimensionless parameters which enter the problem and they will be denoted by

$$\hat{h}_\infty = H_0/D_s = (gH_0^2/\tfrac{1}{2}fQ)^{\frac{1}{2}}, \tag{2.13}$$

$$\hat{H}_r = H_r/D_s = (gH_r^2/\tfrac{1}{2}fQ)^{\frac{1}{2}}, \tag{2.14}$$

$$\hat{R} = \rho_s/w_s \tag{2.15}$$

and

$$\hat{F} = \rho_s/\lambda_s. \tag{2.16}$$

The first two, $\hat{h}_\infty$ and $\hat{H}_r$, are interpreted as upstream parameters and are similar to the upstream parameters of Gill (1977). The last two, $\hat{R}$ and $\hat{F}$, are introduced because of the curvature of the wall and provide a measure of the relative importance of the radius of curvature compared to the radius of deformation and the streamwise length over which the variables vary, respectively. With these definitions (2.4)–(2.7) become

$$\left(1+\hat{R}^{-1}\frac{\hat{n}}{\hat{\rho}}\right)^{-1}\hat{u}\frac{\partial\hat{u}}{\partial\hat{s}}+\hat{v}\frac{\partial\hat{u}}{\partial\hat{n}}+\hat{R}^{-1}\frac{\hat{u}\hat{v}}{\hat{\rho}+\hat{R}^{-1}\hat{n}}-2\hat{h}_\infty\hat{v} = -\left(1+\hat{R}^{-1}\frac{\hat{n}}{\hat{\rho}}\right)^{-1}\hat{h}_\infty\frac{\partial(\hat{h}-\hat{D})}{\partial\hat{s}}, \tag{2.17}$$

$$\left[(\hat{F}\hat{R}^{-1})^2\left\{\left(1+\hat{R}^{-1}\frac{\hat{n}}{\hat{\rho}}\right)^{-1}\hat{u}\frac{\partial\hat{v}}{\partial\hat{s}}+\hat{v}\frac{\partial\hat{v}}{\partial\hat{n}}\right\}\right]-\hat{R}^{-1}\frac{\hat{u}^2}{\hat{\rho}+\hat{R}^{-1}\hat{n}}+2\hat{h}_\infty\hat{u} = -\hat{h}_\infty\frac{\partial(\hat{h}-\hat{D})}{\partial\hat{n}}, \tag{2.18}$$

$$-\frac{\partial\hat{u}}{\partial\hat{n}}+\left[(\hat{F}\hat{R}^{-1})^2\left(1+\hat{R}^{-1}\frac{\hat{n}}{\hat{\rho}}\right)^{-1}\frac{\partial\hat{v}}{\partial\hat{s}}\right]-\hat{R}^{-1}\frac{\hat{u}}{\hat{\rho}+\hat{R}^{-1}\hat{n}} = 2(\hat{h}_\infty-\hat{h}), \tag{2.19}$$

and

$$\tfrac{1}{2}\hat{u}^2+[(\hat{F}\hat{R}^{-1})^2\,\tfrac{1}{2}\hat{v}^2]+\hat{h}_\infty(\hat{h}-\hat{D}) = \hat{h}_\infty\hat{H}_r+2(\hat{\psi}-1). \tag{2.20}$$

The solutions to these equations are subject to the conditions

$$\hat{\psi} = 1, \quad \hat{n} = 0, \tag{2.21}$$

$$\hat{\psi} = 0, \quad \hat{n} = \hat{w} \tag{2.22}$$

and

$$\hat{h} = 0, \quad \hat{n} = \hat{w}. \tag{2.23}$$

As is customary in hydraulic-type problems, variations with downstream distance are assumed to be on a scale large compared to variations across the stream, i.e. $\lambda_s \gg w_s$ or

$$\hat{F}\hat{R}^{-1} \ll 1. \tag{2.24}$$

Accordingly the bracketed terms in (2.17)–(2.20) will be neglected hereafter. Thus the equations decouple and they can be solved for each section s = constant independently. Note that if (2.24) holds true and $\hat{R} \to \infty$, these equations reduce (except for notational discrepancies) to the equations of Gill (1977). This is to be expected, since large $\hat{R}$ entails that variations with downstream distance because of wall curvature are small compared to the effects of other geometrical variations such as a varying bottom topography.

3. The upstream flow

Now consider the upstream flow or the flow as $s \to -\infty$ (the circumflexes will be dropped from here on, except in the parameters $\hat{h}_\infty$, $\hat{H}_r$ and $\hat{R}$). In order to keep the upstream flow as simple as possible, it will be assumed that ρ^{-1} and D both tend to zero in the limit $s \to -\infty$ (i.e. a straight wall and flat bottom). The equations above then correspond to those of Gill (1977) and the solutions can be written in the form

$$h - \hat{h}_\infty = (1 - \hat{h}_\infty)\frac{\cosh(w-2n)}{\cosh w} + \frac{\sinh(w-2n)}{\sinh w}, \tag{3.1}$$

$$u = (1 - \hat{h}_\infty)\frac{\sinh(w-2n)}{\cosh w} + \frac{\cosh(w-2n)}{\sinh w}. \tag{3.2}$$

The width of the flow satisfies the equation

$$t^{-2} + t^2(1-\hat{h}_\infty)^2 + 2(1+\hat{h}_\infty) - 2\hat{h}_\infty \hat{H}_r = 0, \tag{3.3}$$

where

$$t = \tanh w. \tag{3.4}$$

There are two useful numbers which characterize the flow and they will be referred to later in the analysis. These are the Froude number F, defined by

$$F = \overline{u}/(\overline{u} - c), \tag{3.5}$$

and a number r defined by

$$r = \delta u/\overline{u}. \tag{3.6}$$

Here c is the phase speed of long wave disturbances. An overbar denotes the average of the values at the wall and at the free streamline and a δ before the variable is used to denote half the difference between the values at the lateral boundaries. If $F > 1$, the flow is called supercritical and for $F < 1$ the flow is subcritical. The number r is indicative of how much the velocity varies across the stream. If $|r| < 1$, the flow is

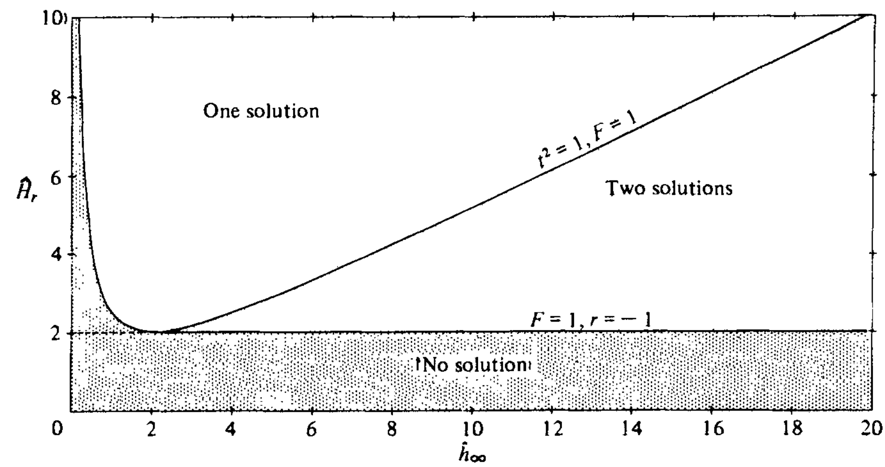

FIGURE 2. The solid curve shows the relation between the upstream parameters $\hat{H}_r$ and $\hat{h}_\infty$ for an infinitely wide current upstream (equation (3.3)]. Below $\hat{H}_r = 2 \cdot 0$ and $\hat{H}_r < 2/\hat{h}_\infty + \frac{1}{2}\hat{h}_\infty$, $\hat{h}_\infty < 2 \cdot 0$ there is no upstream solution. For $\hat{h}_\infty > 2$ and $\hat{H}_r < 2/\hat{h}_\infty + \frac{1}{2}\hat{h}_\infty$, there are two possible solutions, one subcritical, with $F < 1$ and $r < -1$, and one supercritical, with $F > 1$ and $r > -1$. For $\hat{H}_r > 2/\hat{h}_\infty + \frac{1}{2}\hat{h}_\infty$ there is only one solution, which is supercritical, with $F > 1$ and $r > -1$.

unidirectional and positive whereas $r = -1$ indicates that u is zero at the wall (blocking). Proceeding as Gill (1977) we obtain for the two numbers the upstream values

$$F^{-2} = t^2[(1-t^2)\hat{h}_\infty + t^2] \tag{3.7}$$

and

$$r = t^2(1-\hat{h}_\infty). \tag{3.8}$$

In order to obtain a visualization of the possible upstream states figure 2 is constructed. The curves for constant t^2 were obtained by solving (3.3) with respect to $\hat{H}_r$ and plotting $\hat{H}_r$ as a function of $\hat{h}_\infty$ for given t^2. In the region

$$\hat{h}_\infty > 2, \quad 2 < \hat{H}_r < \hat{h}_\infty/2 + 2/\hat{h}_\infty, \tag{3.9}$$

two solutions exist for which $0 < t^2 < 1$. The first is subcritical ($F < 1$) and has a relatively large width and a layer close to the wall where the velocity is negative ($r < -1$). The second is supercritical ($F > 1$), is relatively narrow in width and has unidirectional flow ($-1 < r < 0$). For values of $\hat{H}_r$ larger than

$$\hat{H}_r = 2/\hat{h}_\infty + \hat{h}_\infty/2, \tag{3.10}$$

which corresponds to the curve $t^2 = 1$ of figure 2, there is only one solution for which $t^2 < 1$. This solution is supercritical and unidirectional. The 'critical' value (3.10) represents an upper bound on $\hat{H}_r$ in order for the subcritical inertial boundary current to exist. If $\hat{H}_r$ exceeds this value, a subcritical upstream flow does exist, but in that case the fluid wets both walls of an infinitely wide channel, cf. Gill (1977). There is also a lower bound on $\hat{H}_r$ below which no solutions to (3.3) exist. By (3.2) and (3.3) it follows that

$$u_r^2 = 2\hat{h}_\infty(\hat{H}_r - 2) \tag{3.11}$$

and in order to have real values of the velocity at the wall $\hat{H}_r \geqslant 2$. The different regions and characteristics of the solutions are summarized in figure 2.

The realization of the subcritical upstream flow seems doubtful because of its two-way flow structure. The supercritical one, however, can easily be realized by application of the theory by Gill (1977) to flow in a rotating channel. If the exit channel has slowly varying width and/or depth, the flow is controlled and hence separates from the left wall into a unidirectional boundary current along the right wall downstream. Nevertheless, both types of upstream flows will be discussed below.

If $F = 1$ or if the phase speed of long-wave disturbances is zero upstream, the flow is controlled. Let the subscript c denote controlled flow solutions. Then (3.7) gives

$$t_c^2(1-\hat{h}_\infty) = -1, \tag{3.12}$$

which means that $r = -1$, i.e. that the flow has a stagnation point at the wall. Blocking is recognized if the flow exhibits this feature and therefore even an infinitesimal change in the downstream curvature may cause the flow to be blocked (cf. § 5 below).

4. Dependence of the flow on bottom topography variations

The upstream flow of § 3 will now be assumed to encounter a slowly varying geometry in that the depth and the curvature vary slowly with downstream distance, i.e. (2.24) holds true. The governing differential equations are linear or nonlinear depending on whether or not the wall has irregularities. If the wall is fairly straight, so that $\hat{R}$ is a large number, the equations become linear; this case will be treated first. Moreover, it conveniently serves the purpose of illuminating in a simple way the condition for hydraulic control and the blocking feature.

The topography to be discussed below is chosen to be

$$D = 2\alpha n + D_0, \tag{4.1}$$

where the steepness coefficient α and the weir height D_0 are functions of the downstream co-ordinate such that both α and D_0 tend to zero far upstream. The choice of a linear lateral slope is highly unrealistic for application purposes. However, it is thought to contain most of the important ingredients for an understanding of the behaviour of an inertial boundary current exposed to a varying lateral bottom topography.

In order to obtain an expression which relates the flow variables to the geometry, the procedure of Gill (1977) is followed. When the terms of order $\hat{R}^{-1}$ are neglected in (2.17)–(2.20), the expressions for the fluid depth and velocity become

$$h-\hat{h}_\infty = (\bar{h}-\hat{h}_\infty)\frac{\cosh(w-2n)}{\cosh w}+\delta h\frac{\sinh(w-2n)}{\sinh w} \tag{4.2}$$

and

$$u = \alpha+(\bar{h}-\hat{h}_\infty)\frac{\sinh(w-2n)}{\cosh w}+\delta h\frac{\cosh(w-2n)}{\sinh w}, \tag{4.3}$$

where

$$\bar{h} = \delta h = \tfrac{1}{2}h_r = [1-\alpha\hat{h}_\infty(w-t)+\tfrac{1}{4}(\alpha t)^2]^{\frac{1}{2}}-\tfrac{1}{2}\alpha t. \tag{4.4}$$

The width of the flow is determined by the equation

$$\left(\alpha+\frac{\delta h}{t}\right)^2+t^2(\delta h-\hat{h}_\infty)^2+2[1+\hat{h}_\infty(\delta h-\alpha w-D_0)]-2\hat{h}_\infty\hat{H}_r = 0. \tag{4.5}$$

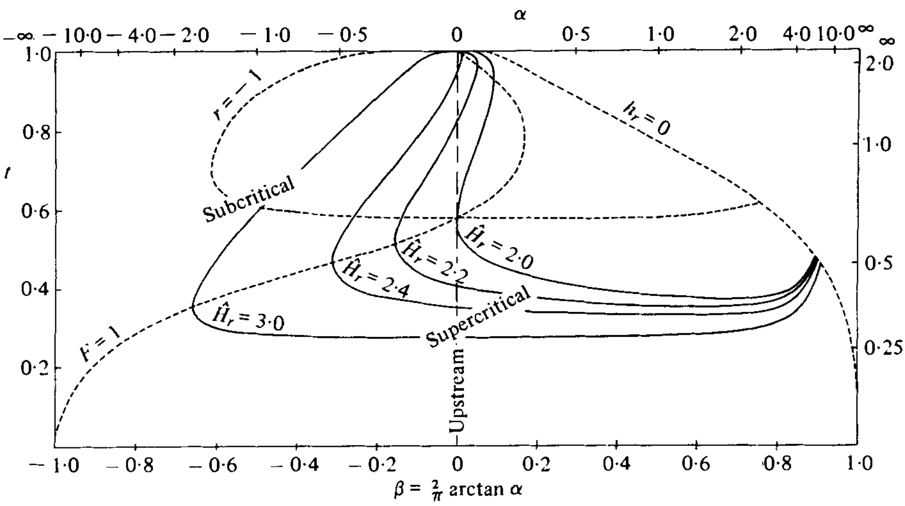

FIGURE 3. Dependence of flow properties on geometry for an inertial boundary current. The geometrical parameter which varies is α, the lateral slope of the bottom ($D_0 = 0$). The solid curves show the relation between the width (in terms of the hyperbolic tangent of the width) and the lateral slope (in terms of $\beta = (2/\pi)\arctan\alpha$) for different values of the parameter $\hat{H}_r$. For comparison the width is indicated to the right and the lateral slope above the figure. The upstream level is $\hat{h}_\infty = 4{\cdot}0$. The broken lines $F = 1$ and $r = -1$ correspond to the locus of the turning points (where branching occurs) and stagnation at the wall, respectively. Curves for other values of $\hat{h}_\infty$ for the case of a straight wall have the same structure.

For $\alpha = D_0 = 0$ this equation reduces to (3.3) and is therefore consistent with the upstream flow. The Froude number and the number r become

$$F^{-2} = \frac{\delta h t^2}{(\alpha t + \delta h)}[(1-t^2)\hat{h}_\infty + t^2 \delta h] \tag{4.6}$$

and

$$r = t^2 \frac{\delta h - \hat{h}_\infty}{\alpha t + \delta h}. \tag{4.7}$$

Equation (4.5) relates the flow properties to geometry in that it gives the flow variable t as a function of the two geometric variables α and D_0 and the two upstream parameters $\hat{h}_\infty$ and $\hat{H}_r$.

For given geometry, $\alpha(s)$ and $D_0(s)$ will be specified, so there will be a specified relation between α and D_0. Substituting in (4.4) and (4.5), a curve relating t to α (or D_0) can be obtained once the upstream parameters $\hat{h}_\infty$ and $\hat{H}_r$ are specified. Figure 3 provides an example of such curves for zero weir height ($D_0 = 0$) and variable steepness, for $\hat{h}_\infty = 4{\cdot}0$. The curves were obtained by solving (4.5) with respect to $\hat{H}_r$, after (4.4) has been used to express δh, and by plotting contours of $\hat{H}_r$ in the t, β plane. Here

$$\beta = \frac{2}{\pi}\arctan\alpha \tag{4.8}$$

has been used to cover the total range of possible α values. All the curves have two branches or more, which reflects the non-linearity of the Bernoulli equation (2.20). The locus of all the turning-points coincides with the curve $F = 1$. This curve is obtained by solving (4.6) with respect to t using an iterative procedure (Newton–

Raphson). To the upper left of this curve the flows are subcritical ($F < 1$) and to the lower right they are supercritical. Inside the looped curve $r = -1$ the flow has a reversed flow layer in the vicinity of the wall.

It turns out that the curves displayed on figure 3 are similar to those which relate the flow variables to the curvature (§ 5). To prepare the way for the discussion of more complex curvature effects on inertial boundary currents, it is useful first to discuss the curves relating the flow variables to bottom topography variations.

If $\alpha = 0$ the only geometric variable is D_0. However, this case has been discussed by Gill (1977) and is therefore omitted here. It is interesting to note, however, that in this case the controlled flow and the blocking of the flow coincide so a discussion of the blocking feature as a separate phenomenon is impossible.

Suppose for instance that the minimum value of β is $-0{\cdot}15$ ($\alpha \simeq -0{\cdot}24$) and that the flow upstream is subcritical (look at the curve $\hat{H}_r = 2{\cdot}4$ for which $t \simeq 0{\cdot}95$ upstream). As β decreases, the width decreases to its value at the constriction ($t \simeq 0{\cdot}72$) without intersecting the curve $r = -1$, i.e. there is always a reversed flow close to the wall. Downstream of the constriction, β increases again. The only continuous solution is the one obtained by retracing the same curve back to $\beta = 0$. For smaller values of $\hat{H}_r$ ($\hat{H}_r = 2{\cdot}2$) the curve $r = -1$ is intersected ($\beta \simeq -0{\cdot}13$, $t \simeq 0{\cdot}58$) before the constriction, so the flow approaching the constriction is unidirectional and subcritical. As the curve is retraced back towards $\beta = 0$ downstream of the constriction, the width increases again until the point where the flow stagnates at the wall ($\beta \simeq -0{\cdot}13$) is reached. At this point a streamline leaves the wall and, if β is increased further downstream, a reversed flow close to the wall is created with streamlines originating downstream (blocked flow). However, a necessary condition for the solution to be physically meaningful is that every streamline can be retraced back to upstream infinity. Thus, the above-created reversed flow is outside the scope of the present theory and the solution breaks down at this point.

For smaller values of $\hat{H}_r$ the solution may be discussed in a similar manner until a curve is reached which has a branch point at $\beta = -0{\cdot}15$. For this 'critical' value of $\hat{H}_r$ a change of branch is possible at the constriction. If this occurs the width continues to decrease even though β is increasing downstream of the constriction. The essential properties of these curves are the branching structure, which allows for hydraulic control, and the intersection of the curves with the curve $r = -1$, which allows the flow to have a stagnation point at the wall at sections which do not coincide with the controlled section.

The section at which control occurs can be found *a priori*. This is due to the fact that the locus of all the turning-points or branch points coincide with the 'critical' curve $F = 1$. Thus there is a way of determining the control section without specifying the upstream parameters. In fact this gives a relationship between the upstream parameters which has to be satisfied in order to have controlled flow solutions. However, no such feature is present at the intersection of the curves with the stagnation curve $r = -1$. Hence, no relationship between the upstream parameters emerges in this case. The event can however involve breakdown of the theory as described above. This point will be returned to in § 6.

5. Dependence of the flow variables on wall irregularities

Consider now that the wall has a non-zero curvature and that $D = 0$ (flat bottom) downstream, i.e. the flow encounters either a bay or a cape. If the characteristic downstream radius of curvature ρ_s is large compared to the radius of deformation, the parameter $\hat{R}$ is large (small curvature). A formal expansion of the dependent variables in terms of this parameter is then possible, viz.

$$(u, v, h, w, \psi) = \sum_{n=0}^{\infty} (u_n, v_n, h_n, \psi_n)\,\hat{R}^{-n}. \tag{5.1}$$

However, if $\hat{R} \sim 1$ (i.e. the bay or cape has a radius of curvature of order 1 radius of deformation) such an approach is impossible. The governing differential equations then in general become nonlinear, which makes them difficult to handle analytically.

Small curvature approach

The zero-order terms in the expansion (5.1) are the upstream solution as described in § 3. Thus for sufficiently small curvatures the upstream values of the flow variables are conserved downstream or, in the presence of a varying bottom topography, behave as described in § 4. The next order in (5.1) therefore contains information about the dependence of the flow variables on curvature.

Substituting (5.1) in (2.17)–(2.20) and collecting terms of order $\hat{R}^{-1}$ gives the following equations:

$$u_0\frac{\partial u_1}{\partial s} - 2h_0 v_1 = -\hat{h}_\infty \frac{\partial h_1}{\partial s}, \tag{5.2}$$

$$2\hat{h}_\infty u_1 = -\hat{h}_\infty \frac{\partial h_1}{\partial s} + \frac{u_0^2}{\rho}, \tag{5.3}$$

$$\frac{\partial u_1}{\partial n} + 2h_1 = -\frac{u_0}{\rho} \tag{5.4}$$

and

$$u_0 u_1 + \hat{h}_\infty h_1 = 2\psi_1, \tag{5.5}$$

subject to the conditions

$$\psi_1 = 0, \quad n = 0, w_0 \tag{5.6}$$

and

$$h_1 - 2w_1 u_0 = 0, \quad n = w_0. \tag{5.7}$$

Proceeding as Gill (1977), the governing equation in terms of ρh_1 becomes

$$\frac{\partial^2}{\partial n^2}(\rho h_1) - 4\rho h_1 = F(n), \tag{5.8}$$

where

$$F(n) = 2u_0[1 - 2\hat{h}_\infty^{-1}(h_0 - \hat{h}_\infty)]. \tag{5.9}$$

Equation (5.8) is solved in the appendix. The deviation from the upstream width times the radius of curvature can be written in the form

$$\rho w_1 = (F_0^2 - 1)^{-1} G(t_0; \hat{h}_\infty, \hat{H}_r). \tag{5.10}$$

Thus the deviation from the upstream width is proportional to $(F_0^2 - 1)^{-1}$ and hence, for non-zero values of the function G, becomes large (of order $\hat{R}$) for upstream parameter values close to those of controlled and blocked upstream flows, so the formal expansion (5.1) breaks down at this point. Moreover, ρw_1 changes sign for $F_0 = 1$, so, if for given values of $\hat{h}_\infty$ and $\hat{H}_r$ the subcritical flow shrinks at bays, the supercritical flow widens (assuming that G conserves its sign). The behaviour of the flow is discussed further below where effects of large curvatures are considered and where the equations are solved by a numerical method.

Large curvatures

When $\hat{R}$ is of order 1 there is no point in making a distinction between ρ_s and w_s in (2.9). In that case all terms in (2.17)–(2.20) are of equal order (except those in brackets). Note that if one assumes that $\hat{h}_\infty$ is large (in which case a large family of subcritical upstream flows exist, cf. § 3) and that ρ is of order 1 or larger, linear differential equations are obtained since the nonlinear ageostrophic term in (2.18) becomes small (of order $\hat{h}_\infty^{-1}$). The resulting linear but ageostrophic differential equation for the fluid depth can be shown to be the governing equation for the modified Bessel functions of order zero (Abramowitz & Stegun 1964, § 9.6). By application of the procedure described in Gill (1977), it is possible to obtain an equation relating the flow variables to the curvature for this case. Below follows, however, a solution of (2.17)–(2.20) by a numerical method (Runge–Kutta) which covers the whole range of possible upstream parameter values. A discussion of large $\hat{h}_\infty$ is, therefore, deferred.

If a new variable ξ is introduced to substitute for n, namely

$$\xi = w - n, \tag{5.11}$$

(2.18) and (2.19) become ($\hat{R} = 1$)

$$dh/d\xi = 2u - u^2\hat{h}_\infty^{-1}(\rho + w - \xi)^{-1}, \tag{5.12}$$

and

$$du/d\xi = 2(h - \hat{h}_\infty) + u(\rho + w - \xi)^{-1}. \tag{5.13}$$

The solution to these equations is subject to three conditions, namely (2.21), (2.22) and (2.23). Combination of (2.20), (2.22) and (2.23) gives two 'initial' ($\xi = 0$) conditions, namely

$$h = 0, \quad u = (2\hat{h}_\infty \hat{H}_r - 4)^{\frac{1}{2}}, \quad \xi = 0, \qquad (5.14), (5.15)$$

where the sign corresponds to a positive value of u at the free streamline (a negative value of u at the free streamline is not consistent with the upstream condition). For given values of $\hat{h}_\infty$ and $\hat{H}_r$, (5.12) and (5.13) are solved to give profiles of surface elevation and velocity at any specified section ρ = constant and for any specified width w. Now, by combination of (2.20) and (2.21), the third condition to be satisfied becomes

$$\tfrac{1}{2}u^2 + \hat{h}_\infty(h - \hat{H}_r) = 0, \quad \xi = w, \tag{5.16}$$

which corresponds to satisfying the Bernoulli equation (2.20) at the wall. In general the solution to (5.12) and (5.13) subject to (5.14) and (5.15) does not satisfy (5.16). Nevertheless, by applying an iterative procedure (e.g. Newton–Raphson), curves like those depicted in figure 4 for $\hat{h}_\infty = 4{\cdot}0$ are obtained for which all three conditions are satisfied. The figure is constructed in much the same way as figure 3. The quantity $t_\rho = \tanh(\rho^{-1})$ is introduced to cover the infinite range of possible curvatures.

Because of the singularity for $\xi = \rho + w$, introduced by the ageostrophic terms in (5.12) and (5.13), a restriction is imposed on w *versus* ρ. Now $0 < \xi < w$, so the

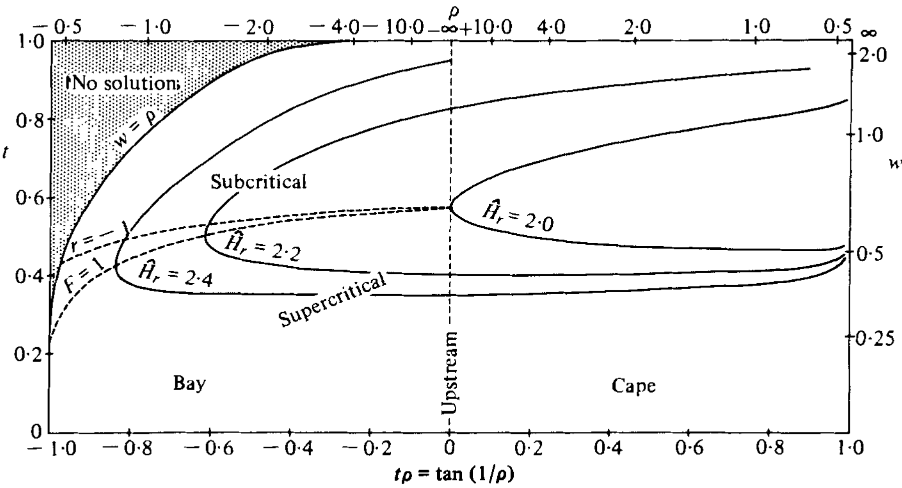

FIGURE 4. Examples of curves relating the flow variable t, the hyperbolic tangent of the width, to the geometric parameter t_ρ, the hyperbolic tangent of the curvature of the wall. The bottom in this case is flat. As in figure 3, $\hat{h}_\infty = 4{\cdot}0$, and the broken lines $F = 1$ and $r = -1$ have the same interpretation.

singularity is avoided if, for negative values of ρ, i.e. at bays, the width is less than the absolute value of the radius of curvature, i.e., if

$$w < |\rho|, \quad \rho < 0. \tag{5.17}$$

The dotted region of figure 4 corresponds to values which do not satisfy this requirement.

The curves obtained in this way are similar to those of figure 3 and may be discussed in the way described in § 4. The essential property of these curves, which allow for hydraulic control, is the existence of two branches. The sections along the coast, which serve as constrictions in the hydraulic sense, are those classified as bays ($\rho < 0$). The branching structure of the curves is present for all values of the upstream parameter $\hat{h}_\infty$.

For reasonable curvatures the curves are strikingly parallel and horizontal in the supercritical domain (i.e. to the lower right of the locus of turning-points). This feature is present for all values of $\hat{h}_\infty$, but is predominant for larger values of $\hat{h}_\infty$, except close to the branch points. Thus for supercritical flows the dependence of the flow variables on wall irregularities is in general weak.

All subcritical upstream flows, i.e. flows for which the upstream parameters satisfy (3.9) and $F < 1$, decrease their width at bay sections and increase their width at cape sections. For supercritical flows, however, there exists a 'critical' value of $\hat{H}_r$ (obtained by setting the function G of (5.10) to zero). For $\hat{H}_r$ less than this critical value, the width at bays (capes) tends to increase (decrease) but tends to decrease (increase) if $\hat{H}_r$ is greater than this value (look at the curves $\hat{H}_r = 2{\cdot}2$ and $\hat{H}_r = 2{\cdot}4$ for which $t = 0{\cdot}40$ and $t = 0{\cdot}35$ upstream respectively).

The blocking feature, in that the flow stagnates at the supporting wall as described in § 4, is also present (shown by the curve $r = -1$ of figure 4). The control section and the section for which the flow is blocked are not clearly separated. If a supercritical

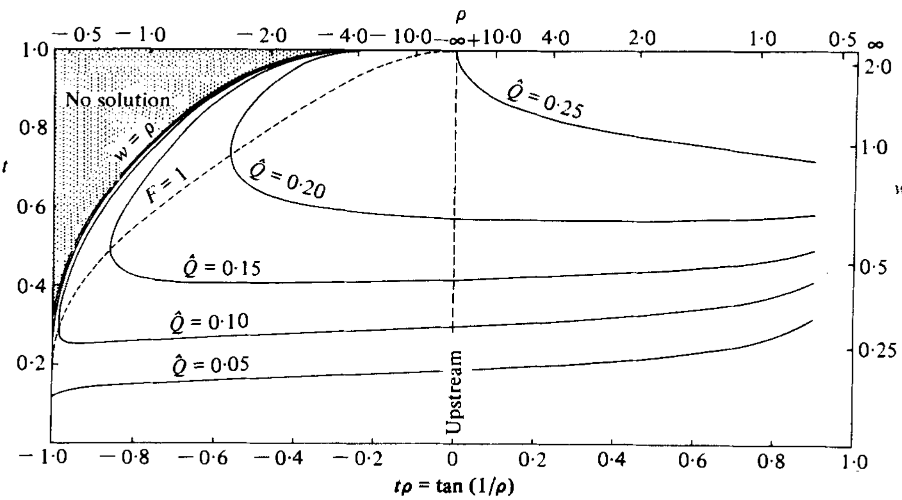

FIGURE 5. The solid curves show the relation between the flow variable t and the geometric parameter t_ρ for flows which satisfy $\hat{h}_\infty = \hat{H}_r$, i.e. flows which in the upstream basin are entirely along the left wall. The variable upstream parameter is the flow rate $\hat{Q} = \frac{1}{2}fQ/gH_0^2 = \hat{h}_\infty^{-2}$.

flow goes subcritical at a bay constriction, the flow becomes blocked shortly downstream of the constriction and the solution breaks down. The second blocking feature, for which the flow separates from the supporting wall (not depicted in figure 4), occurs for very large curvatures at cape sections only, e.g. for $\hat{h}_\infty = 4{\cdot}0$ and $\hat{H}_r = 2{\cdot}4$, the flow separates for $\rho = 0{\cdot}23$ ($t_\rho > 0{\cdot}999$). The curvature effects are further discussed in §§ 6 and 7 below.

6. Some sample configurations

The controlled channel flows discussed by Gill (1977) and verified experimentally by Shen (1978) all predict downstream flows entirely along the right wall. The stream occupies only a part of the channel downstream and so has an effective width less than the channel width, i.e. the remainder of the channel floor will be dry. This kind of flow meets the requirements of the present theory and the evolution of the flow downstream of the control section of the channel is then determined by the results of § 5 above. According to Gill (1977), the most useful application of the theory of the channel flows occurs when the flow in the upstream basin is entirely along the left wall. In that case the fluid depth in the undisturbed part of the basin is kept at its initial level. Then the potential vorticity height and the Bernoulli height are equal, in which case the upstream parameters $\hat{h}_\infty$ and $\hat{H}_r$ are also equal. The flow is then specified by two dimensional upstream parameters only, namely the discharge Q and the fluid depth in the quiescent part of the upstream basin. Downstream of the control section, where the flow separates from the left wall, the present theory applies. The results, for the case when the right wall has irregularities, are depicted in figure 5 in contours of the non-dimensional discharge rate

$$\hat{Q} = \tfrac{1}{2}fQ/gH_0^2 = \hat{h}_\infty^{-2}. \tag{6.1}$$

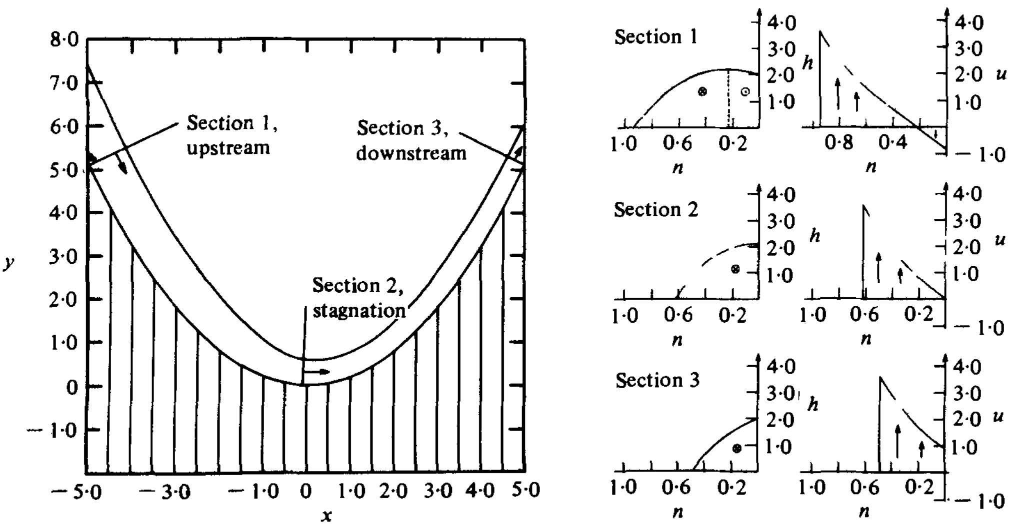

FIGURE 6. Controlled flow solution showing the width as viewed from above and selected profiles of fluid depth and velocity of an inertial boundary current flowing along a parabolic wall. The flow is determined by the upstream parameters which are $\hat{h}_\infty = 4{\cdot}0$ and $\hat{H}_r = 2{\cdot}1$. The profiles are at sections $x = -5{\cdot}0$, $-0{\cdot}09$ and $+5{\cdot}0$ which correspond to radii of curvatures $\rho/\rho_s = -28{\cdot}68$, $-2{\cdot}46$ and $-28{\cdot}68$. The bottom is flat in this case, at level zero. The minimum radius of curvature is $\rho/\rho_s = -2{\cdot}45$ at $x = 0$ where the flow branches.

According to § 3, there is an upper bound to the discharge in order for the inertial boundary current to exist, and it follows from (3.10) that

$$\hat{Q} \leqslant \tfrac{1}{4}, \tag{6.2}$$

in confirmation of the results by Gill (1977). The dashed curve, which intersects the contours at the branching-points, corresponds to flows controlled by the bay constriction ($F = 1$). Figure 5 has some straightforward properties; for instance, the discharge decreases as the curvature increases at the control section.

Figure 6 gives an idea of how the flow properties change as the flow encounters a bay. Since the scaling introduced in § 2 is not fixed for a fixed geometry, it is convenient to discuss figure 6 in terms of dimensional quantities. For this purpose, let x and y be a Cartesian co-ordinate system chosen such that the irregular wall is given by the formula

$$f(x)/\rho_s = \tfrac{1}{2}\alpha(x/\rho_s)^2, \tag{6.3}$$

where α is a constant. Then

$$\rho/\rho_s = -\alpha^{-1}[1+(\alpha x/\rho_s)^2]^{\frac{3}{2}}. \tag{6.4}$$

To construct the controlled flow solution of figure 6, the constant α is tuned such that for the specified values of $\hat{h}_\infty$ and $\hat{H}_r$ the minimum value of $|\rho/\rho_s|$ (i.e. for $x = 0$) equals the corresponding branch point value. The displayed width, x, y and the lateral co-ordinate n are all scaled by ρ_s, whereas the fluid depth h and the velocity u are scaled by

$$d_s = (f\rho_s/4)^2/g, \quad u_s = f\rho_s/8, \tag{6.5}$$

respectively. The plot is for $\hat{h}_\infty = 4{\cdot}0$ and $\hat{H}_r = 2{\cdot}1$, which gives a fairly high potential vorticity. Three profiles of fluid depths and velocity are shown at three different sections: the upstream section, the section at which the current stagnates at the wall and the downstream section. Upstream the flow is subcritical and has a reversed flow close to the wall. This structure remains downstream. However, the reversed flow layer becomes thinner and finally vanishes at the section where the flow stagnates at the wall. Thus, some of the flow towards the bay has returned *via* the reversed flow layer (*c.* 17 %). The flow which approaches the head of the bay is therefore unidirectional. Here, the flow branches and continues as a narrow, unidirectional and supercritical flow downstream of the head of the bay.

Figure 6 can also be interpreted mirrored, i.e. the upstream flow may be the supercritical one. Interpreted this way the flow is blocked shortly after the control section and the solution breaks down. Presumably a kind of turbulent motion, possibly in the form of a hydraulic jump, occurs and propagates upstream. However, it cannot propagate upstream of the constriction where the flow is supercritical. The 'jump' is, therefore, stationary and situated at the constriction. Downstream of the jump an organized motion possibly reappears; this can be computed by applying the usual discontinuity conditions at the jump, i.e. conservation of momentum and discharge. Further sample configurations are discussed below.

7. Discussion

The analysis above shows some steady solutions for an inertial boundary current bounded by a rotating wall to the right of the direction of the mean flow. The response of this flow to changes in the wall curvature and bottom configuration is investigated. The investigation does not give information about how such a flow might be set up, or indeed whether such a current would ever be set up from given initial conditions. However, as mentioned in the introduction the present theory might help to answer some important questions concerning coastal currents or deep currents along continental shelves in the oceans.

(i) May a coastal current be controlled by wall irregularities, or

(ii) is it possible to block the current by such irregularities?

(iii) How large curvature is required at a cape in order for a boundary current to separate from its supporting wall, or

(iv) does the width of the current decrease or increase at sections along the coast where there is a cape (or a bay)?

Problems (i) and (ii) have been discussed in § 6 above and depicted in figure 6. It was shown that a bay of sufficiently large curvature may control the flow in the hydraulic sense. A bay also provides a blocking mechanism for the inertial boundary current. The pertinent discussion of problems (iii) and (iv) may be found in § 5. In order to translate these results into a picture of a flow, figure 7 is constructed. In figure 7 (*a*) a *subcritical* flow encounters a sinusoidal wall as shown. The width of the flow is seen to increase at capes and decrease at bays. The accompanying reversed flow layer behaves accordingly. As the width decreases the flow accelerates in order to keep up with the constant discharge rate. Figure 7 (*b*) illustrates a *supercritical* flow which encounters a cape. The cape has a radius of curvature which is too small for the flow to be able to follow. Thus the whole fluid separates from its supporting wall, at which point the theory breaks down. The little 'bump' at the head of the bay appears since the radius of curvature of the bay is so small that the flow nearly branches there.

The assumptions made in reaching these conclusions may seem too rough to make

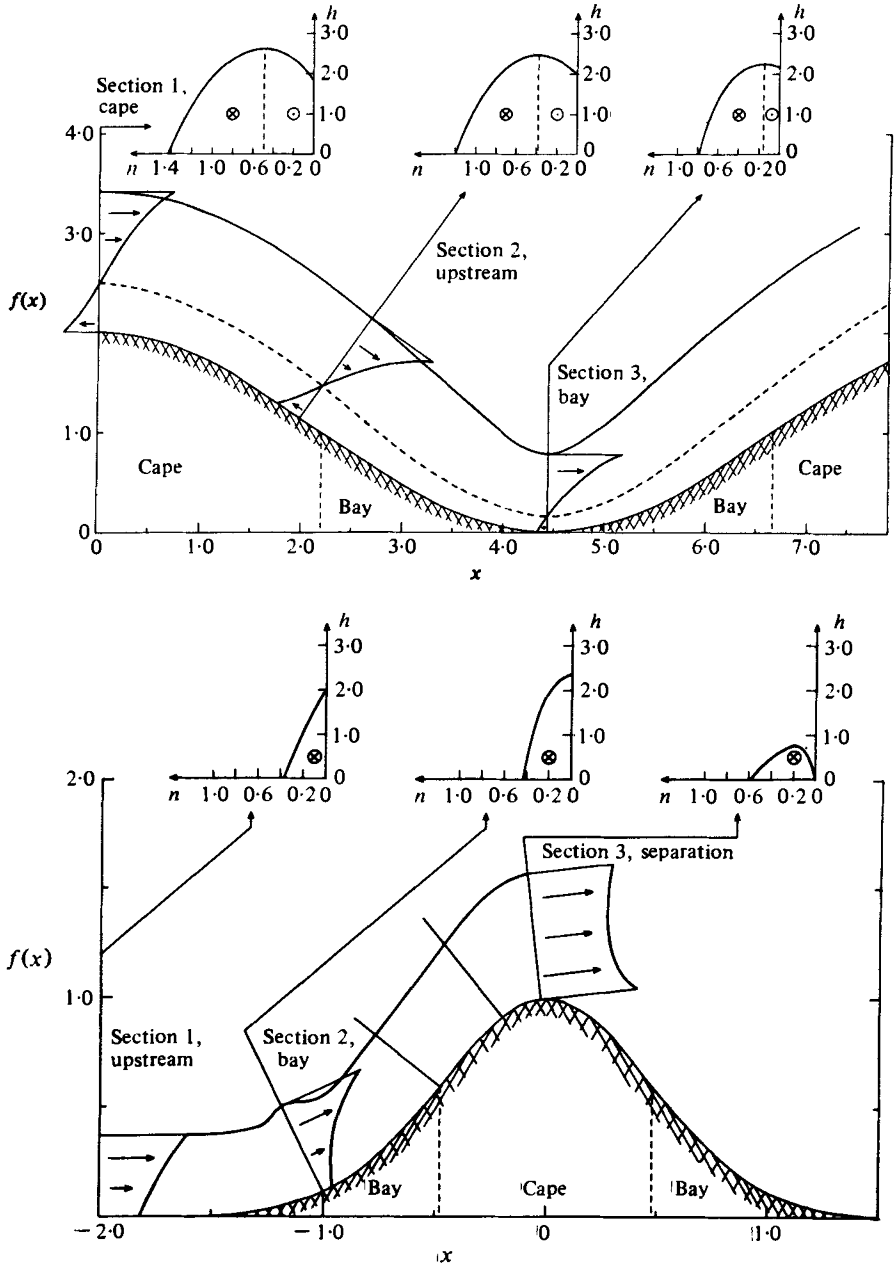

FIGURE 7. Sample configurations of flows along an irregular wall. The flow is viewed from above. Also shown are selected profiles of fluid depth and velocity. The upstream parameters are $h_\infty = 4{\cdot}0$ and (a) $\hat{H}_r = 2{\cdot}2$ and (b) $\hat{H}_r = 2{\cdot}4$. In (a) the wall is sinusoidal, i.e. $f(x) = \rho_s \sin(x/\rho_s\sqrt{2})$ and the flow is subcritical. In this case a reversed flow layer close to the wall appears. In (b) the wall is given by the formula $f(x) = \rho_s \exp(-\kappa x^2/\rho_s^2)$, where $\kappa = 2{\cdot}2$, and the flow is supercritical. For explanation of the symbols see §6. For further details see §7.

useful inferences to actual oceanic cases. For instance, the one-layer assumption, which can be overcome in a two-layer model if one of the layers is quiescent, is not relevant in most shallow coastal waters, where there usually are two distinct layers which both move. However, regarding the possibility of controlled flows at bays, it is interesting to note that the outlined features shown in figure 6 are similar to the coarse features, observed by Sundby (1978), of the in/out flow of surface waters in the Vestfjorden, i.e. a broad two-way stream enters the fjord at one side and leaves as an intense unidirectional stream at the other side.

The flows discussed in the present paper are all boundary currents supported by a wall to the right of the direction of the mean flow (Northern Hemisphere). However, as some exploratory investigations have shown, the method used above is also applicable to flows in inertial boundary layers supported by a wall to the left of the direction of the mean flow. This kind of model may give insight into problems pertaining to separation and possible blocking of western boundary currents such as the Gulf Stream.

Appendix

Equation (5.8) is the generating equation for hyperbolic functions. Using the standard method of variation of parameters the solution can be written

$$\rho h_1 = I(n) + (\rho\bar{h}_1 - \bar{I})\,\frac{\cosh(w-2n)}{\cosh w} + (\delta\rho h_1 + \bar{I})\,\frac{\sinh(w-2n)}{\sinh w}. \tag{A 1}$$

Here

$$I(n) = \frac{1}{2}\int_0^n F(\xi)\sinh 2(n-\xi)\,d\xi, \tag{A 2}$$

where $F(\xi)$ is given by (5.9). By applying (5.5), (5.6) and (5.7)

$$\rho w_1 = (F_0^2 - 1)^{-1}\,G(t_0; \hat{h}_\infty, \hat{H}_r). \tag{A 3}$$

The function G is given by

$$G = [1 + F_0^2 t_0^2(2 + t_0^2)]\,C_1 - [1 + F_0^2(1 + t_0^2)]\,C_2 + (1 + F_0^2\,t_0^2)(\hat{H}_r - 2), \tag{A 4}$$

where

$$C_1 = \frac{w\hat{h}_\infty}{4t_0} + \frac{4\hat{h}_\infty r_0 + (18 - 3\hat{h}_\infty)\,\hat{h}_\infty - 16}{12\hat{h}_\infty(1 - t_0^2)} \tag{A 5}$$

and

$$C_2 = \frac{w}{4t_0}(1 - r_0) + \frac{(1 + r_0)(3\hat{h}_\infty - 1 - r_0) + 1 - t_0^2}{12\hat{h}_\infty(1 - t_0^2)}. \tag{A 6}$$

I should like to thank Professor M. E. Stern for introducing me to the problems of hydraulic control in presence of rotation and for many stimulating discussions on the subject.

Part of this work was supported by the National Science Foundation and Office of Naval Research for Summer Programs in Geophysical Fluid Dynamics at Woods Hole Oceanographic Institution. The support is gratefully acknowledged.

REFERENCES

ABRAMOWITZ, M. & STEGUN, I. A. 1964 *Handbook of Mathematical Functions*. Washington: National Bureau of Standards.

GILL, A. E. 1977 *J. Fluid Mech.* **80**, 641.

ROUSE, H. 1961 *Fluid Mechanics for Engineers*. Dover.

SAMBUCO, E. & WHITEHEAD, J. A. 1976 *J. Fluid Mech.* **73**, 521.

SHEN, C. Y. 1978 The rotating hydraulics of steady flow in open channels. Ph.D. thesis, University of Rhode Island.

STERN, M. E. 1972 *Phys. Fluids* **15**, 2062.

STERN, M. E. 1974 *Geophys. Fluid Dyn.* **6**, 127.

STERN, M. E. 1976 *Ocean Circulation Physics*. Academic.

SUNDBY, S. 1978 Coun. Meet. Int. Coun. Explor. Sea (C: 51).

WHITEHEAD, J. A., LEETMAA, A. & KNOX, R. S. 1974 *Geophys. Fluid Dyn.* **6**, 101.